ChemComm

Accepted Manuscript

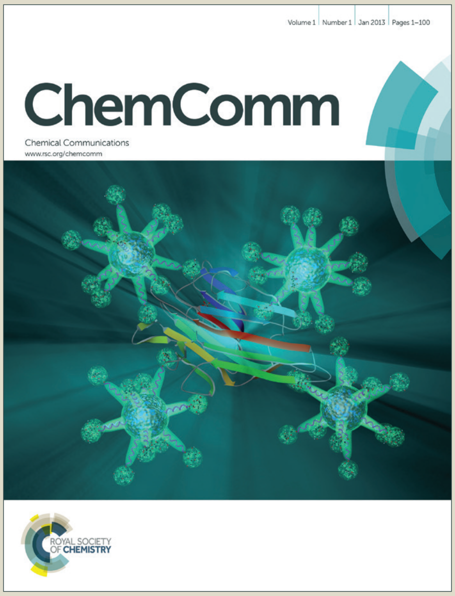

ROYAL SOCIETY OF CHEMISTRY

www.rsc.org/chemcomm

Journal Name

RSCPublishing

COMMUNICATION

Cite this: DOI: 10.1039/x0xx00000x

Electron-spin excitation by implanting hydrogen to metallofullerene: the synthesis and spectroscopic characterizations of $Sc_4C_2H@I_h$-C_{80}

Received 00th January 2012,
Accepted 00th January 2012

DOI: 10.1039/x0xx00000x

www.rsc.org/

Yongqiang Feng,[a] Taishan Wang,*[a] Jingyi Wu,[b] Zhuxia Zhang,[a] Li Jiang,[a] Hongbin Han,*[c] and Chunru Wang*[a]

A hydrogen-containing endohedral metallofullerene, $Sc_4C_2H@I_h$-C_{80}, was synthesized and its paramagnetism was measured by the low-temperature EPR spectrometry with a broad EPR signal. The electron-spin excitation by implanting H-atom would be a new method for preparation of stable paramagnetic metallofullerenes.

The paramagnetic metallofullerenes with unpaired spin(s) have potential applications in quantum information processing and electronic devices, etc.[1-3] As many metallofullerenes are diamagnetic, the electron spin injection becomes an important way to produce spin-active species, e.g., the technique by electrochemical redox or chemical reduction with alkali-metals.[4-7] However, this technique would produce either anion or cation radicals of the metallofullerenes, which are obviously not stable and apt to return to their diamagnetic states spontaneously. Therefore, it is necessary to investigate other method to excite paramagnetic property of metallofullerenes.

In 2007, Dunsch et al. reported an endohedral metallofullerene, $Sc_3CH@C_{80}$, in which the H forms covalent bonding with C and supplies an electron as revealed by theoretical calculations.[8] Although the resulted $Sc_3CH@C_{80}$ is diamagnetic molecule, the existence of this stable metallofullerenes suggests the possibility to implant hydrogen into the metallofullerenes accompanied with an extra electron. Therefore, introducing H-atom to diamagnetic endohedral metallofullerenes could also realize electron spin excitation.[9]

However, it requires a lot of energy to insert an atom into the metallofullerene cage, so the H-containing paramagnetic metallofullerenes were synthesized by arc-discharging the metal-doped graphite with introducing a certain amount of hydrogen gas into the helium atmosphere. After deliberately comparing the metallofullerene products before and after introducing the hydrogen gas in the arc-discharging process, a new species with 1165 molecular weight was discovered in the presence of hydrogen. Furthermore, along with the increasement of hydrogen ratio in the helium gas, the yield of this molecule increases simultaneously. Therefore, this molecule with 1165 molecular weight was supposed to be a H-containing endohedral metallofullerene. In addition, since the molecule with 1165 molecular weight has a nearly same retention time with the known $Sc_4C_2@I_h$-C_{80} (1164 molecular weight)[10] in the high performance liquid chromatography (HPLC) profile, so the relativity between these two species was proposed as well. Herein, we report the isolation, characterizations, and theoretical calculations of this new molecule of $Sc_4C_2H@I_h$-C_{80}. UV-vis, Raman, IR, and ESR spectroscopies as well as density functional theory (DFT) calculations were employed to disclose its structure and special electronic property. The structural and electronic properties of $Sc_4C_2@I_h$-C_{80} were also analyzed for comparison.

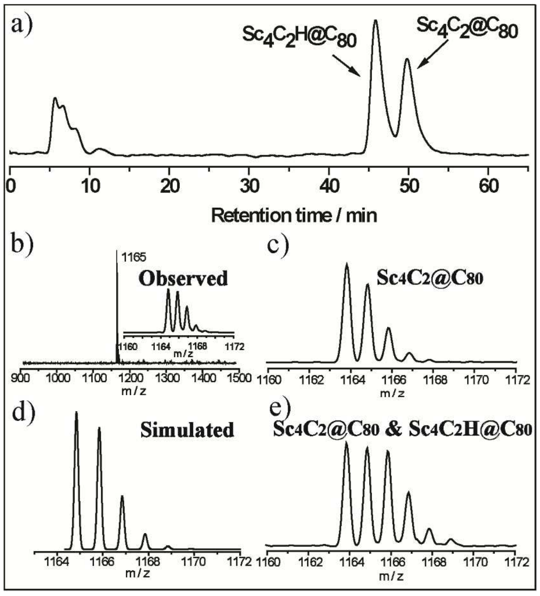

Figure 1. (a) HPLC separation profile of $Sc_4C_2H@C_{80}$ and $Sc_4C_2@C_{80}$; (b) Observed mass spectrum of purified $Sc_4C_2H@C_{80}$; (c) Observed molecular ion peak of purified $Sc_4C_2@C_{80}$; (d) Simulated isotropic distributions of $Sc_4C_2H@C_{80}$; (e) Mass spectrum of a mixture of $Sc_4C_2@C_{80}$ and $Sc_4C_2H@C_{80}$.

$Sc_4C_2H@I_h$-C_{80} was synthesized through arc-discharging method under a mixture atmosphere of 6 Torr H_2 and 194 Torr He. The produced fullerenes and metallofullerenes were isolated by multi-step HPLC, as shown in Figure 1a and S1. It can be seen that the $Sc_4C_2H@I_h\text{-}C_{80}$ has similar retention time with that of $Sc_4C_2@I_h\text{-}C_{80}$ on HPLC columns. In addition, the $Sc_4C_2H@I_h\text{-}C_{80}$ and $Sc_4C_2@I_h\text{-}C_{80}$ have slightly shorter time than that of $Sc_3N@I_h\text{-}C_{80}$,[11] revealing their similar molecular size and polarity. The MALDI-TOF mass spectra shown in Figure 1b exhibit mass-to-charge ratio (m/z) of 1165 for $Sc_4C_2H@C_{80}$, accounting for a chemical composition of $Sc_4C_{82}H$ whose simulated isotropic distributions are in good agreement with the experimental result. In order to obtain the accurate m/z of $Sc_4C_{82}H$, purified $Sc_4C_2@C_{80}$ sample was added as internal standard. The main molecular ion peaks at 1164 and 1165 in Figure 1e are attributed to $Sc_4C_2@C_{80}$ and $Sc_4C_{82}H$, respectively.

To elucidate the structure of $Sc_4C_{82}H$, spectroscopic characterizations were performed. It is generally acknowledged that the UV-Vis-NIR spectrum of metallofullerene is mainly related to the π-π* transitions, which are determined by the cage size and symmetry as well as the electronic structure.[1,12] The onset wavelength of the $Sc_4C_{82}H$ is 933 nm (see Figure S4 in ESI), corresponding to an energy gap of 1.33 eV. Other absorption peaks present at 670, 416, and 335 nm. For comparison, the onset value of $Sc_4C_2@I_h\text{-}C_{80}$ was found at 969 nm and the optical band-gap was estimated to be 1.28 eV.[10] Moreover, the resembling features of these two absorption spectra indicate that the $Sc_4C_{82}H$ has similar $I_h\text{-}C_{80}$ carbon cage.

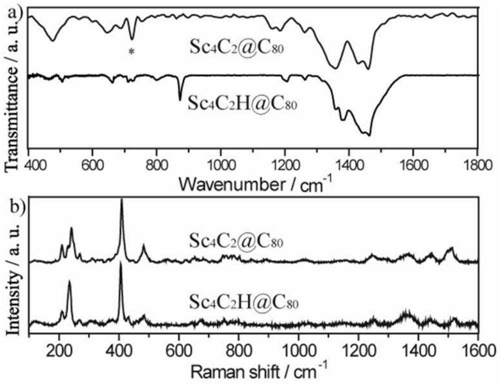

Figure 2. (a) FTIR spectra and (b) low-energy Raman (laser wavelength 633 nm) spectra of $Sc_4C_2@C_{80}$ and $Sc_4C_2H@C_{80}$. The asterisk refers to some impurity.

Figure 2 shows the IR and Raman spectra of $Sc_4C_2H@C_{80}$. For comparison, the vibration spectra of $Sc_4C_2@I_h\text{-}C_{80}$ were also exhibited. It is known that in IR spectrum the vibration frequencies between 1000 and 1600 cm^{-1} belong to the fingerprint peaks of cage-derived modes.[13,14] Such characteristic tangential vibrations of $Sc_4C_2H@C_{80}$ were observed at 1460, 1380, 1356, and 1262 cm^{-1} as shown in Figure 2a. These tangential vibrations resembles to the corresponding modes in $Sc_4C_2@I_h\text{-}C_{80}$ as well as in other $M_3N@I_h\text{-}C_{80}$ (M = Sc, Y, Dy, Gd) with $I_h\text{-}C_{80}$ carbon cage.[1,13,14] The asymmetrical $Sc\text{-}C_{carbide}$ vibrations appeared at 711 and 662 cm^{-1}, which also resemble those of $Sc_4C_2@I_h\text{-}C_{80}$.[10] Figure 2b shows the Raman spectra of $Sc_4C_2H@C_{80}$ and $Sc_4C_2@I_h\text{-}C_{80}$. Similar as their IR spectra, the Raman spectra of these two compounds exhibit analogous pattern, further confirming their similarity in cage symmetry and endohedral moiety. And the lines at about 407 and 233 cm^{-1} feature the $I_h\text{-}C_{80}$ modes as well as the endohedral Sc-C stretching modes.

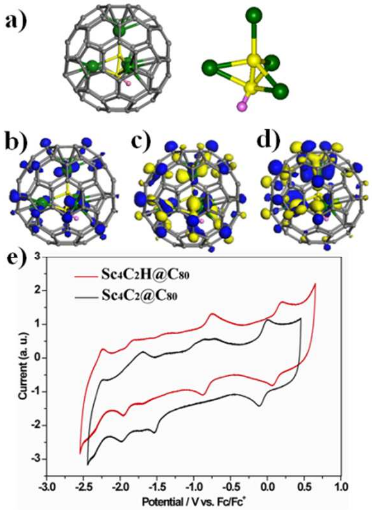

Figure 3. (a) DFT-optimized structure; (b) spin density distributions (blue parts); (c) SOMO; and (d) LUMO orbitals of $Sc_4C_2H@C_{80}$. (H: pink, Sc: green, $C_{carbide}$: yellow, C_{cage}: gray); (e) CV curves of $Sc_4C_2H@C_{80}$ (red) and $Sc_4C_2@C_{80}$ (black) measured in *o*-dichlorobenzene with 0.05 M $TBAPF_6$ at a glassy carbon working electrode referring to saturated calomel electrode.

DFT calculations were executed to describe the $Sc_4C_2H@C_{80}$ in detail. Figure 3a shows the optimized structure of $Sc_4C_2H@I_h\text{-}C_{80}$, which possesses a similar structure with $Sc_4C_2@I_h\text{-}C_{80}$ except for a bonded hydrogen atom. Briefly, the outer cage is an $I_h\text{-}C_{80}$ cage; four scandium atoms form a tetrahedron encaging C_2 unit. The bonded H to C_2 unit forms a hydrocarbon moiety, which resembles to that in $Sc_3CH@I_h\text{-}C_{80}$.[8] For comparison, other isomers of $Sc_4C_2@C_{80}H$ with hydrogen bonding to the cage were calculated. However, these isomers are 46.20~162.72 kJ/mol less stable than optimized $Sc_4C_2H@I_h\text{-}C_{80}$.

Detailed analyses of Kohn-Sham molecular orbitals reveal that $Sc_4C_2H@I_h\text{-}C_{80}$ has a valence state of $[Sc_4C_2H]^{6+}@[C_{80}]^{6-}$, in which the $[Sc_4C_2H]^{6+}$ cluster consists of one Sc^{2+} cation, three Sc^{3+} cations, C_2^{6-} anion and H^+ cation. The optimal C-C bond length of the central C_2^{6-} moiety in $Sc_4C_2H@I_h\text{-}C_{80}$ is 1.479 Å, comparable to that of the C_2^{6-} in $Sc_4C_2@I_h\text{-}C_{80}$ (1.478 Å).[10] The calculated C-H bond length in C_2H unit is 1.09 Å. And the shortest Sc-H bond length (2.29 Å) in $Sc_4C_2H@I_h\text{-}C_{80}$ is comparable to that in $Sc_3CH@I_h\text{-}C_{80}$ (2.11 Å),[8] but much longer than that in other scandium hydride compounds, such as ScH_3 (1.8 Å).[15] In $Sc_4C_2H@I_h\text{-}C_{80}$, its nearest $Sc\text{-}C_{carbide}$ distance (1.97 Å) is much shorter than the nearest $Sc\text{-}C_{cage}$ distance (2.23 Å).

The bonding parameters in $Sc_4C_2H@I_h\text{-}C_{80}$ and $Sc_4C_2@I_h\text{-}C_{80}$ are listed in Table 1. It can be seen that the introduction of H influences the geometry of Sc_4C_2 cluster obviously. Although the C-C bond length is similar, the $Sc\text{-}C_{carbide}$ bond length in $Sc_4C_2H@C_{80}$ is slightly longer than the corresponding $Sc\text{-}C_{carbide}$ bond in $Sc_4C_2@C_{80}$, indicating enlarged scandium tetrahedron by introducing one hydrogen atom.

Table 1. Selected bonding parameters (Å) in $Sc_4C_2H@C_{80}$ and $Sc_4C_2@C_{80}$.

	Sc-Sc[a]	Sc-C[a]	C-C	Sc-H	C-H
$Sc_4C_2H@C_{80}$	3.21-3.75	1.97-2.27	1.47	2.29, 2.37	1.09
$Sc_4C_2@C_{80}$	3.26-3.54	1.97-2.14	1.48		

[a] Bond length ranging from the shortest to the longest.

As shown in Figure 3c and 3d, both of the singly occupied molecular orbitals (SOMOs) and the lowest unoccupied molecular orbitals (LUMOs) mainly reside on the endohedral Sc_4C_2H cluster and partly on the cage. For reported $Sc_4C_2@I_h\text{-}C_{80}$ anion state, the added electron is mostly localized on the $I_h\text{-}C_{80}$ cage.[16] In $Sc_4C_2H@I_h\text{-}C_{80}$, the H also supplies an electron; however, its unpaired spin mainly locates on the Sc_4 cluster. Therefore, it can be seen that the introduction of covalently bonding H not only influences the geometry of endohedral cluster but also greatly changes the molecular electronic structure.

The electrochemical property of $Sc_4C_2H@C_{80}$ was then investigated, as shown in Figure 3e. For $Sc_4C_2H@C_{80}$, its first oxidation potential appears at 0.20 V and three reduction peaks were observed at −0.87, −1.68, −1.95 V; whereas in $Sc_4C_2@C_{80}$, the first oxidation potential appears at 0.01 V and two reduction peaks exhibit at −1.53 and −1.97 V, respectively.

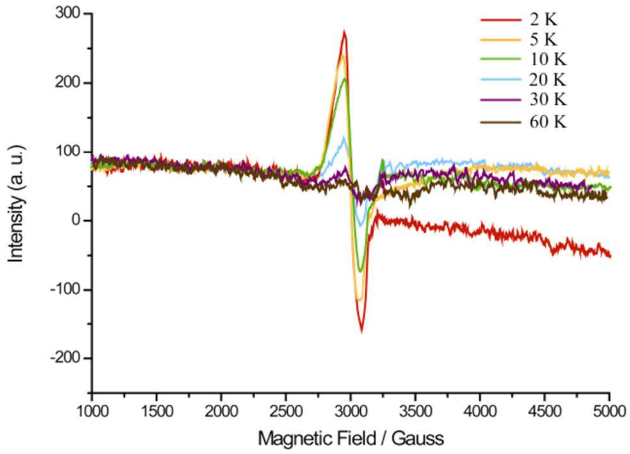

Figure 4. EPR spectra of $Sc_4C_2H@C_{80}$ in CS_2 measured at low temperatures.

DFT calculation results revealed that the $Sc_4C_2H@I_h\text{-}C_{80}$ has open-shell electronic structure. Then the EPR characterizations were performed, strangely, no obvious EPR line was observed for $Sc_4C_2H@I_h\text{-}C_{80}$ solution at room temperature.

However, when the temperature was decreased down to 60 K, a distinguishable EPR line was detected. Moreover, with further decreasing sample temperature, the ESR peak intensity increased greatly, as shown in Figure 4. At 2 K, the EPR signal has a line width of about 500 G. Although there is no hyperfine coupling splitting, the large peak width indicates strong spin-metal couplings and Sc(3*d*)-based unpaired spin distributions. Similar phenomenon was also observed in EPR spectrum of $TiSc_2N@I_h\text{-}C_{80}$,[17] in which a broad signal (~250 G) with no splitting was obtained at 100 K.

This type of EPR spectra can be ascribed to the significant anisotropy of the *g* tensor, which may be caused by the embedded electron spins in $Sc^{2+}(3d^1)$ and $Ti^{3+}(3d^1)$. As shown in Figure 3b, the calculated spin density distributions of $Sc_4C_2H@I_h\text{-}C_{80}$ disclose that its unpaired electron is partly delocalized on the other three $Sc^{3+}(3d)$ orbitals. Considering the above discussed valance states of four Sc cations, the $Sc^{2+}(3d^1)$ ideally bears the major unpaired spin of $Sc_4C_2H@I_h\text{-}C_{80}$. The spin site of $Sc(3d^1)$ was also observed on $Sc_3N@I_h\text{-}C_{80}$ anion[18] and $Sc_4O_2@I_h\text{-}C_{80}$ ion radicals[4]. In addition, in $TiSc_2N@I_h\text{-}C_{80}$ the unpaired spin resides on $Ti^{3+}(3d^1)$ as well.[17]

In summary, this study indicates clearly the existence of stable paramagnetic metallofullerene molecule $Sc_4C_2H@I_h\text{-}C_{80}$, which coexists with the diamagnetic $Sc_4C_2@I_h\text{-}C_{80}$. The electron-spin excitation by implanting H-atom would be an optimal method for preparation of stable paramagnetic metallofullerenes. Since accelerated proton may easily penetrate the fullerene cage, it is expected that the spin excitation may be easily obtained by proton bombarding the metallofullerene as well.

We thank the National Natural Science Foundation of China (21203205, 21121063), National Basic Research Program (2012CB932900), NSAF (11179006, 11076027). We also thank the High Magnetic Field Laboratory of Chinese Academy of Sciences.

Notes and references

[a] *Beijing National Laboratory for Molecular Sciences, Laboratory of Molecular Nanostructure and Nanotechnology, Institute of Chemistry, Chinese Academy of Sciences, Beijing 100190, China. Fax: 86-10-62652120; Tel: 86-10-62652120; E-mail: wangtais@iccas.ac.cn, crwang@iccas.ac.cn*
[b] *Laboratory of Nuclear Analysis Techniques, Institute of High Energy Physics, Chinese Academy of Sciences, Beijing, 100049, China*
[c] *Department of Radiology, Peking University Third Hospital, Beijing 100191, China. E-mail: hanhongbin@bjmu.edu.cn*

† Electronic Supplementary Information (ESI) available: Experimental details, HPLC chromatogram, UV-vis, NMR spectra and DFT calculations. See DOI: 10.1039/b000000x

1 A. A. Popov, S. Yang and L. Dunsch, *Chem. Rev.*, 2013, **113**, 5989.
2 J. Lee, H. Kim, S. J. Kahng, G. Kim, Y. W. Son, J. Ihm, H. Kato, Z. W. Wang, T. Okazaki, H. Shinohara and Y. Kuk, *Nature*, 2002, **415**, 1005.
3 S. Sato, S. Seki, Y. Honsho, L. Wang, H. Nikawa, G. Luo, J. Lu, M. Haranaka, T. Tsuchiya, S. Nagase and T. Akasaka, *J. Am. Chem. Soc.*, 2011, **133**, 2766;
4 A. A. Popov, N. Chen, J. R. Pinzón, S. Stevenson, L. A. Echegoyen and L. Dunsch, *J. Am. Chem. Soc.*, 2012, **134**, 19607.
5 P. Jakes and K.-P. Dinse, *J. Am. Chem. Soc.*, 2001, **123**, 8854.
6 Y. Feng, T. Wang, J. Wu, Y. Ma, Z. Zhang, L. Jiang, C. Ge, C. Shu and C. Wang, *Chem. Commun.*, 2013, **49**, 2148.
7 L. Echegoyen, C. J. Chancellor, C. M. Cardona, B. Elliott, J. Rivera, M. M. Olmstead and A. L. Balch, *Chem. Commun.*, 2006, 2653.
8 M. Krause, F. Ziegs, A. A. Popov and L. Dunsch, *ChemPhysChem*, 2007, **8**, 537.
9 A. Dankert, R. S. Dulal and S. P. Dash, *Sci. Rep.*, 2013, **3**, 3196.
10 T.-S. Wang, N. Chen, J.-F. Xiang, B. Li, J.-Y. Wu, W. Xu, L. Jiang, K. Tan, C.-Y. Shu and X. Lu, *J. Am. Chem. Soc.*, 2009, **131**, 16646.
11 S. Stevenson, Rice, G., Glass, T., Harich, K., Cromer, F., Jordan, M. R., Craft, J., Hadju, E., Bible, R., Olmstead, M. M., Maitra, K., Fisher, A. J., Balch, A. L. Dorn, H. C., *Nature*, 1999, **402**, 898.
12 A. A. Popov, S. M. Avdoshenko, A. M. Pendás and L. Dunsch, *Chem. Commun.*, 2012, **48**, 8031.
13 M. Krause, H. Kuzmany, P. Georgi, L. Dunsch, K. Vietze and G. Seifert, *J. Chem. Phys.*, 2001, **115**, 6596.
14 S. Yang, S. I. Troyanov, A. A. Popov, M. Krause and L. Dunsch, *J. Am. Chem. Soc.*, 2006, **128**, 16733.
15 A. H. Neuhaus, E. D. Glendening and A. Streitwieser, *Organometallics*, 1996, **15**, 3688.
16 K. Tan, X. Lu and C.-R. Wang, *J. Phys. Chem. B*, 2006, **110**, 11098.
17 A. A. Popov, C. Chen, S. Yang, F. Lipps and L. Dunsch, *ACS nano*, 2010, **4**, 4857.
18 A. A. Popov and L. Dunsch, *J. Am. Chem. Soc.*, 2008, **130**, 17726.

Table of Contents

A spin-active hydrogen-containing metallofullerene, $Sc_4C_2H@C_{80}$, with nested structure was synthesized and investigated.